DOI: 10.1002/ejic.200701331

Hybrid Organic–Inorganic Porphyrin–Polyoxometalate Complexes

Clémence Allain,[a,b] Sophie Favette,[a] Lise-Marie Chamoreau,[a] Jacqueline Vaissermann,[a] Laurent Ruhlmann,*[b] and Bernold Hasenknopf*[a]

Keywords: Polyoxometalates / Porphyrinoids / N ligands / Electrochemistry / Supramolecular chemistry

Two Anderson-type polyoxomolybdates $[FeMo_6O_{18}\{(OCH_2)_3CNHCO(4\text{-}C_5H_4N)\}_2]^{3-}$ and $[MnMo_6O_{18}\{(OCH_2)_3CNHCO(4\text{-}C_5H_4N)\}_2]^{3-}$ and two Lindqvist-type polyoxovanadates $[V_6O_{13}\{(OCH_2)_3CCH_2OC(O)(4\text{-}C_5H_4N)\}_2]^{2-}$ and $[V_6O_{13}\{(OCH_2)_3CNHCO(4\text{-}C_5H_4N)\}_2]^{2-}$ were functionalized with pendant pyridyl groups. The electrochemical analysis revealed reversible redox processes at the heteroatom of the Anderson-type compounds and at the vanadium atoms in the Lindqvist series. Axial coordination of the polyoxometalate-grafted pyridyl groups to the metal ion in [Ru(CO)TPP] (TPP = tetraphenylporphyrin) and [ZnTPP] yielded polyoxometalate–porphyrin assemblies in solution. Evidence for electronic communication between the polyoxometalate and the porphyrin was established by fluorescence spectroscopy. Cyclic voltammetry showed the influence of the porphyrin on the redox process of the polyoxometalate and also nucleophilic attack at the porphyrin skeleton by the pendant pyridyl groups. Implications for the construction of supramolecular functional devices based on these components are discussed.

Introduction

The modular construction of supramolecular assemblies from molecular components is a current strategy for the preparation of functional devices.[1] In a typical set-up, molecules with specific properties are selected as building blocks. Once the molecules are assembled, their properties complement each other to yield an integrated functional material. Metalloporphyrins are attractive components in materials because of their appealing chemical and photochemical properties: high stability, intense visible absorption bands, long-lived excited states, and tunability by chemical derivatization.[2] Thus, with appropriate metal ions, they are well suited as electron donors, and they are often used in supramolecular systems.[3] On the other hand, polyoxometalates (POMs) are a class of inorganic compounds containing metals in high oxidation states – mainly W^{VI}, Mo^{VI}, and V^{V} – and are known to behave as electron reservoirs.[4] The combination of porphyrins with POMs in one supramolecular entity may yield a promising arrangement capable of forming charge-separated states by photoinduced electron transfer.[5]

[a] UPMC Univ Paris 06, Institut de Chimie Moléculaire FR2769, Laboratoire de Chimie Inorganique et Matériaux Moléculaires UMR CNRS 7071, case courrier 42,
4 place Jussieu, 75252 Paris Cedex 05, France
Fax: +33-1-44-27-38-41
E-mail: Bernold.Hasenknopf@upmc.fr
[b] Université Paris-Sud 11, Laboratoire de Chimie Physique UMR CNRS 8000, Bâtiment 350,
91405 Orsay Cedex, France
Fax: +33-1-69-15-43-28
E-mail: laurent.ruhlmann@lcp.u-psud.fr

Supporting information for this article is available on the WWW under http://www.eurjic.org or from the author.

Supramolecular aggregates between POMs and metalloporphyrins by electrostatic interactions and/or coordination to the POM framework have been prepared[6] and used as oxidation catalysts[7] or for electrocatalytic reductions.[8] Although such assemblies are easy to prepare and rather robust, neither the relative orientation of the components nor the stoichiometry are under control. The covalent linkage of photosensitizer and POM is a way to overcome this problem.[9] Alternatively, their assembly by directional interactions, such as coordination bonds, allows formation of structures with a greater degree of order. Axial ligation to metalloporphyrins has been commonly employed to build designed architectures.[2a] For example, the assembly of a donor–acceptor porphyrin–fullerene system was realized by the grafting of an N-heterocycle to the fullerene and subsequent coordination to the metal ion in a porphyrin.[10] Inspired by this approach, we designed a family of POMs functionalized by pendant pyridyl ligands that act as electron-acceptor molecules together with porphyrin donors in a supramolecular assembly. We present here the preparation and characterization of such systems.

Results and Discussion

Functionalized POMs Bearing Pyridine Groups

The ligands $(HOCH_2)_3CNHCO(4\text{-}C_5H_4N)$ (**1**) and $(HOCH_2)_3CCH_2OC(O)(4\text{-}C_5H_4N)$ (**2**) linking a triol moiety to a pyridyl group by an amide or ester bond were synthe-

sized following procedures adapted from Newkome et al.[11] and Stevens,[12] respectively. Functionalized POM $[FeMo_6O_{18}\{(OCH_2)_3CNHCO(4\text{-}C_5H_4N)\}_2]^{3-}$ (**3**, Anderson-Fe-pyridine) was prepared by the reaction of $[N(C_4H_9)_4]_4[\alpha\text{-}Mo_8O_{26}]$ with $Fe(acac)_3$ and **1** in refluxing acetonitrile, following our published procedure.[13] $[MnMo_6O_{18}\{(OCH_2)_3CNHCO(4\text{-}C_5H_4N)\}_2]^{3-}$ (**4**, Anderson-Mn-pyridine) was obtained by the same procedure by using $Mn(CH_3COO)_3$ to introduce the heteroatom and has been previously reported by us.[14] Because Lindqvist-type POMs are known for their reversible electrochemical behavior,[15] we also prepared functionalized Lindqvist hexavanadate compounds. $[V_6O_{13}\{(OCH_2)_3CCH_2OC(O)(4\text{-}C_5H_4N)\}_2]^{2-}$ (**5**, Lindqvist-ester-pyridine) was synthesized by reaction of decavanadate $[N(C_4H_9)_4]_3[H_3V_{10}O_{28}]$ with **2** in refluxing acetonitrile, following the procedure described by Zubieta et al.[15] The same procedure with triol derivative **1** gave the expected polyanion $[V_6O_{13}\{(OCH_2)_3CNHCO(4\text{-}C_5H_4N)\}_2]^{2-}$ (**6**, Lindqvist-amide-pyridine), albeit with a very low yield (4%). The conditions described by Hill et al.[16] allowed a substantial increase in the yield (44%). All POMs **3**–**6** were isolated as tetrabutylammonium salts.

The compounds were characterized by single-crystal X-ray diffraction. Crystal structure data of **3** and **5** are summarized in Table 3, **4**[14] and **6**[16] (see also Supporting Information) were previously published. The molecular structure of the anion **3** is very similar to that of **4**. Both compounds are δ isomers of the Anderson polyanion,[17] with a trisalkoxo ligand on each side. Compounds **5** and **6** are Lindqvist-type polyanions, in which the six vanadium atoms form an octahedron. The two trisalkoxo ligands occupy opposite faces of the octahedron, as observed in analogous compounds previously reported.[15,16] The functionalized POM **5** is centrosymmetric, with the six vanadium atoms equivalent, which is not the case for our crystals of **6**. However, the differences between the subsequently reported structure of **6** by Hill and our structure are not important, and we did not pursue this X-ray analysis further. In the compounds **3**–**6**, the pyridine rings are not involved in metal binding (Figure 1). The pyridyl nitrogen atoms are separated by ca. 2 nm.

The IR spectra of compounds **3**–**6** (listed in the Experimental Section) are in agreement with those of POM structures. For compound **3**, the $\nu_{Mo=O}$ band at 664 cm^{-1} (667 cm^{-1} for **4**), and $\nu_{Mo-O-Mo}$ at 941, 923 and 906 cm^{-1} (942, 921, 903 cm^{-1} for **4**) are characteristic of the Anderson structure. The $\nu_{C=O}$ band at 1667 cm^{-1} (1671 cm^{-1} for **4**) and ν_{C-O} at 1029 cm^{-1} (1026 cm^{-1} for **4**) attest to the presence of the organic ligand and its fixation on the polyoxometalate core. For compound **5**, the bands at 952 cm^{-1} ($\nu_{V=O}$), 809, and 721 cm^{-1} ($\nu_{Mo-O-Mo}$) correspond to the Lindqvist structure. The bands at 1735 cm^{-1} ($\nu_{C=O}$), 1136, and 1061 cm^{-1} (ν_{C-O}) attest to the grafting of the ester **2** onto the POM. In an analogous manner, compound **6** presents bands at 955, 811, and 723 cm^{-1} that are typical of the Lindqvist structure and at 1669, 1101, and 1049 cm^{-1}, which indicate the presence of the organic ligand.[16]

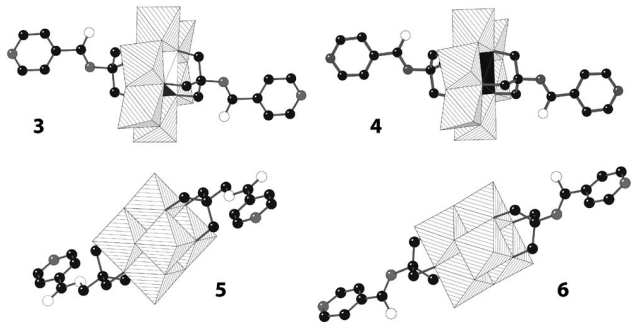

Figure 1. Structures of polyoxometalates bearing free pyridyl groups: $[FeMo_6O_{18}\{(OCH_2)_3CNHCO(4\text{-}C_5H_4N)\}_2]^{3-}$ (**3**), $[MnMo_6O_{18}\{(OCH_2)_3CNHCO(4\text{-}C_5H_4N)\}_2]^{3-}$ (**4**), $[V_6O_{13}\{(OCH_2)_3CCH_2OC(O)(4\text{-}C_5H_4N)\}_2]^{2-}$ (**5**), $[V_6O_{13}\{(OCH_2)_3CNHCO(4\text{-}C_5H_4N)\}_2]^{2-}$ (**6**).

The compounds were also investigated by ^1H NMR spectroscopy. Compounds **3** and **4** are paramagnetic, and strong line broadening is observed for the signals of the tetrabutylammonium cations. Signals for the organic ligands are observed only for compound **4**. Grafting of the organic ligand onto the POM is evidenced by a broad singlet at δ = 64.4 ppm for the CH_2O group. The pyridyl hydrogen atoms give rise to signals in the normal range (δ = 8.65 and 7.65 ppm) without fine coupling. In contrast, for diamagnetic compounds **5** and **6**, chemical shifts of the CH_2O group are in the normal range 5.2–5.3 ppm. For compound **5**, one has to notice that the single signal observed in the ^{51}V NMR spectrum (δ = –499 ppm) confirms the equivalence of the six vanadium atoms shown by the crystal structure, and this value is in agreement with the literature value of –495 ppm for **6**.

Electrochemistry

The electrochemical behavior of compounds **3**–**6** was investigated in organic solution by cyclic voltammetry (CV). Electrochemical data are gathered in Table 1, and typical cyclic voltammograms are presented in Figure 2. All compounds exhibit quasireversible redox processes: the cathodic peak currents (and anodic for **4**) are almost proportional to the square root of the scan rate from 10 to 500 $mV\,s^{-1}$ (see Figure 2 insets), which indicates that the processes are diffusion-controlled.

The reductions at ca. –0.5 V observed for compounds **5** and **6** (Figure 2) are in agreement with literature data for Lindqvist-type anions bearing tris(oxymethylmethane) ligands.[15,18] This quasireversible redox behavior is typical of type I polyanions.[19] Controlled-potential coulometry at the potential of the reduction processes yielded ca. 1.1 electrons exchanged per functionalized POM **6**, which demonstrates that the reduction process involves one electron.

Anderson-type anions **3** and **4** are type II anions, and reduction of d^0 molybdenum to d^1 is expected to be irreversible. Thus, it can be hypothesized that the first reversible redox activities of **3** and **4** are centered on the heteroatom, Fe and Mn, respectively. Controlled-potential

Table 1. Electrochemical data for compounds **3**, **4**, **5**, and **6**.[a]

Compound	Solvent	$E°'_1$	$E°'_2$	$E°'_3$
Anderson-Fe-pyridine **3**	CH_3CN	–1.55[irr]	–0.75	
	1,2-$C_2H_4Cl_2$/CH_3CN (1:1)	–1.41[irr]	–0.66	
Anderson-Mn-pyridine **4**	CH_3CN	–1.98	–0.65	0.82
	1,2-$C_2H_4Cl_2$/CH_3CN (1:1)	–[b]	–0.59	0.85
Lindqvist-ester-pyridine **5**	dmf	–1.88[irr]	–0.49	
Lindqvist-amide-pyridine **6**	CH_3CN	–1.15[irr]	–0.38	
	dmf	–1.32[irr]	–0.49	
	1,2-$C_2H_4Cl_2$/CH_3CN (1:1)	–[b]	–0.31	

[a] Data obtained from cyclic voltammetry (scan rate 100 mV/s). Analyte concentration: 0.5 mM, with 0.1 M $TBAPF_6$ as electrolyte. $E°'$, approximated by $(E^a_p + E^c_p)/2$, are given in V vs. SCE. [b] Not observed.

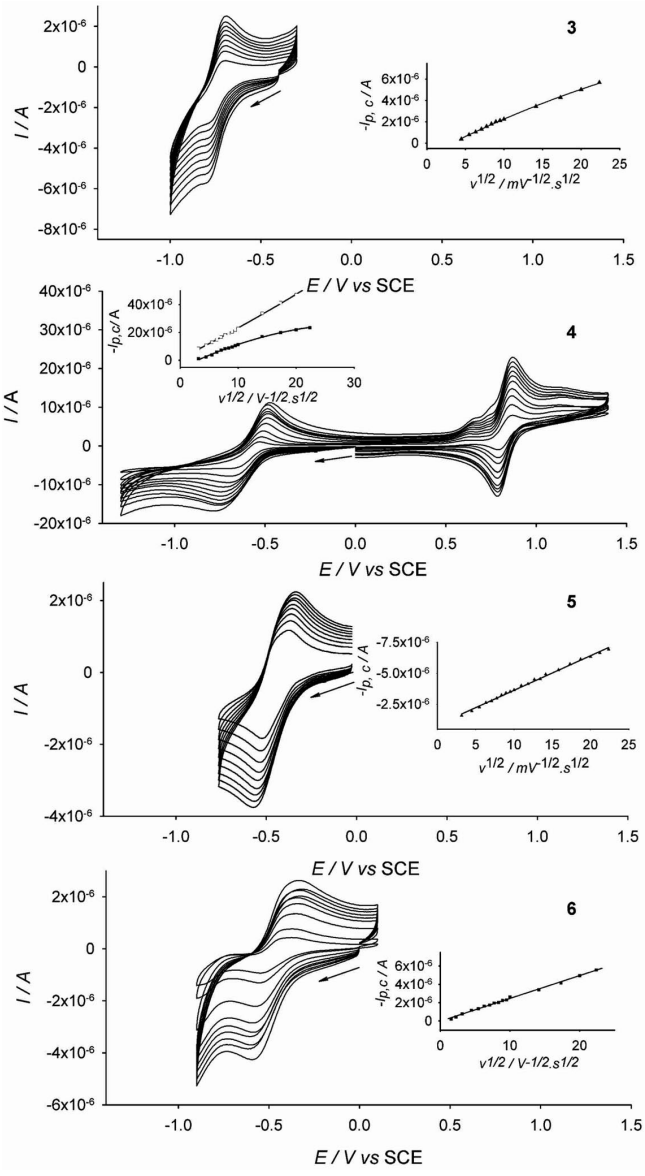

Figure 2. Cyclic voltammograms of compounds **3** and **4** in CH_3CN and **5** and **6** in dmf (top to bottom, concentration 0.5 mM) with 0.1 M $TBAPF_6$ as electrolyte at different scan rates (20–100 mV s^{-1}). Inset: plot of the peak current versus square root of the scan rate; for **4**: (■) reduction process and (□) oxidation process.

coulometry indicated the exchange of one electron per redox process. The second cathodic process is effectively irreversible, which is in agreement with the reduction of the molybdenum heteroatom.

In addition to the cathodic waves discussed above, the manganese species **4** also shows an anodic process at +0.83 V (Figure 2). Surprisingly, controlled-potential coulometry at +1.00 V resulted in the passage of 2.2 electrons per complex. This is in apparent contradiction with the cyclic voltammogram presented in Figure 2, from which comparison of the peak current of the anodic and cathodic processes indicates that only one electron seems to be exchanged. This might be explained by the oxidation of Mn^{III} to Mn^{IV}, which in turn would react with itself by disproportionation to form 0.5 equiv. manganese(V) and 0.5 equiv. of the starting manganese(III) species. This species would then be oxidized again at the electrode to manganese(IV). In the end, such disproportionation would result in the passage of 2 electrons and the formation of a manganese(V) species.[20]

POM–Porphyrin Coordination Complexes

We decided to investigate the ability of compounds **3**–**6** to form coordination complexes with ruthenium(II) and zinc(II) *meso*-tetraphenylporphyrins [Ru(CO)TPP] and [ZnTPP]. These two porphyrins are monovacant complexes in the sense that they easily accept one further ligand, such as the nitrogen atom of a pyridine ring. Decarbonylation of [Ru(CO)TPP(pyridine)] complexes by irradiation liberates a further coordination site, and the construction of polymers might be possible in combination with POMs **3**–**6**.[21] These metalloporphyrins are neutral and therefore should avoid non-specific charge interactions with the POM. They display interesting photophysical properties (luminescence for [ZnTPP] and possibility of photoinduced electron transfer for [Ru(CO)TPP]).

Titrations of [Ru(CO)TPP] (10^{-5} M in $CHCl_3$, 1% CH_3CN) with **4** or with **5** (10^{-3} M in CH_3CN) were followed by absorption spectroscopy. Small redshifts were observed for the Soret and the Q bands. These shifts correspond well to the literature data on [Ru(CO)(L)TPP] (L = nitrogen ligands including pyridine) complexes.[22] Axial coordination of the pendant pyridyl groups to the Ru can therefore be

presumed. However, when the titrations were conducted in $CH_3CN/CHCl_3$, spectral changes were not observed either with **4** or with pyridine. In those cases, [Ru(CO)TPP-(CH_3CN)] is the major complex present in the beginning, and its spectral characteristics are close to that of the final pyridine complex. Because CH_3CN is a necessary co-solvent for solubilization of the POMs, the use of absorption spectroscopy is limited.

Addition of a stoichiometric amount of [Ru(CO)TPP] to a solution of **4** in $CHCl_3/CH_3CN$ led, within minutes, to the formation of the complex **4**-[Ru(CO)TPP]$_2$, which was isolated as a red powder by precipitation with diethyl ether. We first characterized this complex by ^{1}H NMR spectroscopy. The two doublets corresponding to the pyridine ring of **4** are considerably shielded: $\Delta\delta$ = –2.37 ppm for H_B and $\Delta\delta$ = –7.3 ppm for H_A (Figure 3). This upfield shift, which arises because of the ring current above the face of the porphyrin, is comparable to that in other axially bound pyridyl ligands.[23] In the spectrum of the complex, protons H_A are masked by the signals of the tetrabutylammonium cations, but selective irradiation of the signal at δ = 1.33 ppm changes the signal for protons H_B into a singlet, which proves that the chemical shift of protons H_A is around 1.3 ppm. In addition, the pairs of *ortho* protons of each porphyrin phenyl ring, which give rise to only one signal in the spectrum of the starting [Ru(CO)TPP], are differentiated upon formation of the complex because of the slower rate of rotation of the *meso* carbon – phenyl carbon bond: protons H_c and $H_{c'}$ appear as two doublets.[24] Complexes between [Ru(CO)TPP] and **5** and **6** show similar characteristics (Figures S1 and S2, Supporting Information). Thus, axial coordination of all three POMs is established.

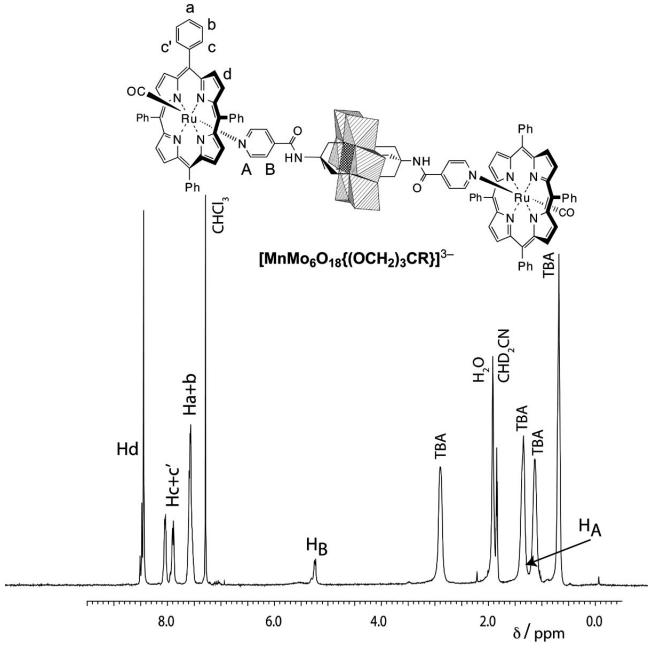

Figure 3. ^{1}H NMR spectra (in $CDCl_3/CD_3CN$) of the complex between **4** and [RuTPP(CO)].

Titrations of **4** and **6** with [Ru(CO)TPP] were followed by ^{1}H NMR spectroscopy (in $CDCl_3/CD_3CN$, Figure 4 and S3). Coordination of the nitrogen of the pyridine ring to the ruthenium atom is expected to be strong: for more than 2 equiv. porphyrin added, only the 2:1 complex is observed. In addition, ligand exchange is slow on the NMR timescale: mono- and di-addition products can be clearly distinguished for less than 2 equiv. porphyrin added. These titrations allow the estimation of the association constant of the complexes: $\beta = 3\times10^8$ M^{-1} for complex **4**-[Ru(CO)-TPP]$_2$ and $\beta = 4\times10^7$ M^{-1} for **6**-[Ru(CO)TPP]$_2$. Thus, in millimolar solutions of stoichiometric amounts of POM (1 equiv.) and [Ru(CO)TPP] (2 equiv.) about 10% of the porphyrin is not coordinated to the POM.

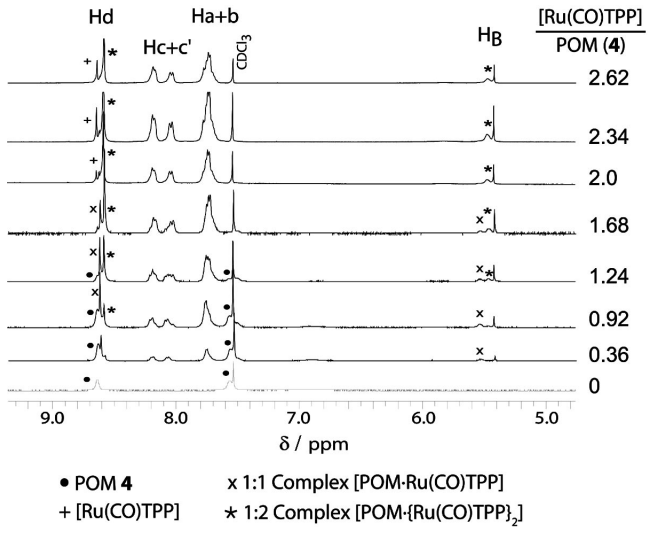

Figure 4. ^{1}H NMR spectroscopic titration (in $CDCl_3/CD_3CN$, 4:6, concentration 4 mM) of compound **4** with [RuTPP(CO)].

Formation of the complexes with [Ru(CO)TPP] was also established by IR spectroscopy: the ν_{C-O} band of [Ru(CO)-TPP] shifts from 1940 cm^{-1} for the free porphyrin to 1948 cm^{-1} for the complex with **3**, to 1951 cm^{-1} with **4**, and to 1953 cm^{-1} with **5**. This shift can be attributed to a stronger back bonding of the ruthenium to the carbonyl and is similar to that described in the literature.[25] Importantly, this shift evidences the axial coordination of POM **3**, for which NMR analysis is impossible because of its paramagnetic nature.

We then investigated the formation of complexes between functionalized POMs **3**–**6** and [ZnTPP]. Titrations of [ZnTPP] with **4** were followed by absorption spectroscopy, and small redshifts of the absorption bands were observed, which indicates axial binding.[26] Yet again, acetonitrile (necessarily present to solubilize the POM) is a competing ligand and [ZnTPP(CH_3CN)] presents a similar spectrum to the pyridine complex.[26] Because zinc forms weaker coordination bonds with nitrogen than ruthenium,[27] spectral changes were observed beyond the molar ratio 2:1 ([ZnTPP]/**4**). The ^{1}H NMR spectrum of the reaction solution of **4** (8.7 mM in $CDCl_3/CD_3CN$, 7:1) with [ZnTPP]

(4 equiv.) shows the shielding of the pyridyl protons of **4**, but to a lesser extent than that observed with [Ru(CO)TPP]: $\Delta\delta$ = –1.64 ppm for H_B and $\Delta\delta$ = –4.97 ppm for H_A. Nevertheless, this shift indicates axial coordination to Zn. The signals corresponding to the porphyrin are not modified by complexation, contrary to that observed for the complexes with [Ru(CO)TPP]. When a titration of **4** with [ZnTPP] is performed (Figure S4), a single series of signals is observed, which shift upon successive additions. Thus, the exchange between free and [ZnTPP]-bound POM is fast on the NMR timescale.[27]

Complexes between POMs **3**–**6** and [ZnTPP] were studied by fluorescence spectroscopy. At micromolar concentrations, a slight quenching of the emission fluorescence spectrum can be noticed in the presence of a large excess of POM. By using a spectrometer with a front-face geometry, the fluorescence of [ZnTPP] at 5 mM was measured in the presence of 0.5 and 1 equiv. of **4** (see Figure S5). A steady decrease in the fluorescence intensity was observed. This indicates an energy-transfer process from the excited porphyrin to the POM. However, at high concentrations, an additional fluorescence band occurs (presumably because of aggregation), and at low concentrations the complexes dissociate if no excess POM is used. This renders a detailed analysis of the photophysical properties of these complexes difficult.

Finally, we investigated the electrochemical properties of the complexes formed by functionalized POMs **3**–**6** with [Ru(CO)TPP] (Table 2). A mixture of acetonitrile/1,2-dichloroethane 1:1 was chosen in order to ensure the solubility of the starting compounds as well as the resulting complex. Figure 5 presents the cyclic voltammograms recorded from a solution of Anderson-Mn-pyridine **4** before and after the addition of [RuTPP(CO)].

Table 2. Electrochemical data for complexes [POM–Ru(CO)TPP].

Complex	$E°'_1$	$E°'_2$	$E°'_3$	$E°'_4$	$E°'_5$
Ru(CO)TPP	*–1.90*	*–1.48*	*0.83*	*1.25*	
Complex **3**-[Ru(CO)TPP]$_2$	–1.33^{irr} *–1.43*	–0.68	*0.87*	*1.29*	*1.61^{irr}*
Complex **4**-[Ru(CO)TPP]$_2$	*–1.46*	–0.69	0.86[b]	*1.29^{irr}*	*1.57^{irr}*
Complex **5**-[Ru(CO)TPP]$_2$	*–1.37*[a] –1.85[a] *–1.99*[a]	–0.59[a]	*1.03^{irr}*[a]		
Complex **6**-[Ru(CO)TPP]$_2$	*–1.44*	–0.30	*0.92*	–	*1.61^{irr}*

[a] Recorded in dmf. Data obtained from cyclic voltammetry (scan rate 100 mV/s). Analyte concentration: 0.5 mM in 1,2-$C_2H_4Cl_2$/CH_3CN (1:1) with 0.1 M $TBAPF_6$ as electrolyte unless otherwise noted. $E°'$, approximated by $(E^a_p + E^c_p)/2$ are given in V vs. SCE. Potential values in italics were observed for Ru(CO)TPP; normal characters for POM. [b] These potentials were observed in both Ru(CO)TPP and POM systems.

One can readily notice that the cyclic voltammogram of the complex is not the sum of the two cyclic voltammograms of the POM and the porphyrin, which implies an interaction between the components of this assembly. The reduction peak potential of POM **4** has shifted to more negative values from –0.59 V (**4**) to –0.69 V (**4**-[Ru(CO)TPP]$_2$) and the process notably slows down upon formation of the

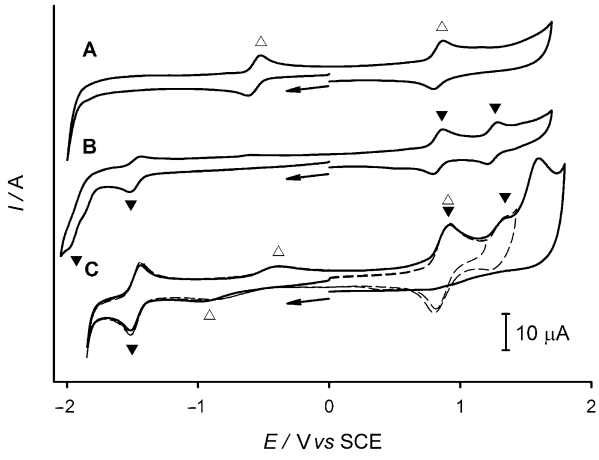

Figure 5. Cyclic voltammograms of compound **4** (A), [RuTPP(CO)] (B), and the resulting coordination complex (C) at 0.5 mM in 1,2-$C_2H_4Cl_2$/CH_3CN (1:1) with 0.1 M $TBAPF_6$ as electrolyte.

complex. This behavior is observed irrespective of the scan direction and scan limits and is therefore evidence of the influence of the porphyrin on the POM in the complex. The first two oxidation peaks, one reversible and the second irreversible, correspond to the π-cation radical and to the formation of the dication of the porphyrin ring of [Ru(CO)-TPP], respectively. These processes occur at the same potentials in the free and POM-bound metalloporphyrin. The irreversible new wave observed at ca. 1.57 V should be attributed to the oxidation of an isoporphyrin,[28,29] which implies a nucleophilic attack at the *meso* position of the porphyrin dication $[Ru(CO)TPP]^{2+}$. Such a process has been studied previously.[29] Our cyclic voltammograms are in good agreement with the previously reported redox behavior of porphyrins in the presence of nucleophiles[30] and, in particular, with the well-documented reports of Himman et al.[28] We suppose that in the present case the nucleophile is the pyridyl group of the functionalized POM **4** that has been liberated by decomplexation from the Ru center. Although the nucleophilic attack could in principle also occur on the π-cation radical generated at the first oxidation potential,[29] this reaction was not detected during our cyclic voltammetric experiments, presumably because its kinetics were too slow.[31]

Similar results were obtained by using the functionalized POMs **3**, **5**, and **6** with [Ru(CO)TPP]. The reduction process on the POM **3** subunit at –0.68 V remarkably slows down upon formation of the complex as for **4**-[Ru(CO)-TPP]$_2$, in contrast to POMs **5** and **6**, which present a quasi-reversible first monoelectronic reduction. We still observed irreversible new waves at ca. 1.6 V for the other POM–porphyrin complexes **3**-[Ru(CO)TPP]$_2$ and **6**-[Ru(CO)TPP]$_2$, which can be attributed to the oxidation of an isoporphyrin formed by nucleophilic attack of the pyridyl substituent in the *meso* position of the macrocycle. In the case of **5**-[Ru(CO)TPP]$_2$, this third irreversible wave as well as the second oxidation process were not observed; the first oxidation was already irreversible.

Conclusions

In summary, we have prepared a series of four polyoxometalates with pendant pyridyl groups. They all present reversible redox processes at potentials that are tuned by the composition of the POMs. The pyridyl nitrogen atoms coordinate to the metalloporphyrins [ZnTPP] and [Ru(CO)TPP]. Thus, supramolecular assemblies can be obtained in solution containing photo- and redox-active building units. Quenching of the [ZnTPP] fluorescence indicates that communication between the individual components exists. However, because of the weak coordination of Zn to the pyridyl nitrogen atoms, the association between the functionalized POM and [ZnTPP] is only partial. Cyclic voltammetric studies of the assemblies with [Ru(CO)TPP] show a change in the reduction potentials and that the reversible redox reactions on the POM become irreversible in the presence of [Ru(CO)TPP]; this, again, is a sign of the influence of the components on each other. Furthermore, we found evidence for the nucleophilic attack of the POM-grafted pyridyl groups at *meso* positions of the porphyrin, which implies decomplexation from the Ru center. Therefore, the usefulness of functional devices constructed by the complexation of pyridines seems to be limited. Stronger association is definitely needed. We are currently pursuing this route by grafting oligodentate ligands on the POMs to enhance complexation stabilities with metal complexes and by linking covalent POMs to porphyrins. Preliminary results indicate a better communication in those cases, and they will be reported in due course.

Experimental Section

General Remarks: $[N(C_4H_9)_4]_4[\alpha\text{-}Mo_8O_{26}]$[32] and $[N(C_4H_9)_4]_3[H_3V_{10}O_{28}]$[33] were prepared by literature methods. Methyl isonicotinate and isonicotinoyl chloride were prepared from isonicotinic acid by standard procedures. Acetonitrile for polyoxometalate synthesis was freshly distilled from CaH_2. All other chemicals, including solvents, were commercially available as reagent grade and used as received. [Ru(CO)TPP] and its complexes were protected from strong light. Elemental analyses were performed by the Service de microanalyse, Université Pierre et Marie Curie, Paris, France and by the Service central d'analyse, CNRS, Vernaison, France.

Spectroscopy: NMR spectra (^1H, ^{13}C, ^{51}V) were recorded with a Bruker AC300 spectrometer at 300, 75.5, and 79 MHz, respectively. Chemical shifts (δ) are expressed in ppm relative to Me_4Si for ^1H and ^{13}C NMR, with the residual solvent peak as standard and relative to 100% $VOCl_3$ for ^{51}V NMR. IR spectra were recorded by using KBr pellets with a Bio-Rad FTS 165 spectrometer at 4 cm^{-1} resolution. Relative intensities are given after the wavenumber as vs = very strong, s = strong, m = medium, w = weak, sh. = shoulder, br. = broad. Steady-state optical absorption spectra were recorded with a Perkin–Elmer Lambda 19 spectrophotometer. Steady-state luminescence emission spectra were obtained by using a Spex fluorolog 111 spectrofluorimeter equipped with a Hamamatsu R3896 photomultiplier that was cooled to a temperature of –20 °C. The fluorescence spectra were not corrected for the response of the detection system. All measurements were carried out at room temperature.

Electrochemical Experiments: Acetonitrile, dmf, and 1,2-dichloroethane used for electrochemical measurements were HPLC grade and were used as received. The analyte concentration was 0.5 mM. The electrolyte was tetrabutylammonium hexafluorophosphate ($TBAPF_6$), 0.1 M. The solutions were deaerated thoroughly by bubbling argon through the solution and kept under argon atmosphere during the whole experiment. The source, mounting and polishing of the glassy carbon electrode (GC, Tokai, Japan) have been described previously.[34] The glassy carbon electrodes had a diameter of 3 mm. The electrochemical apparatus EG&G 273A was driven by a personal computer. Potentials are quoted versus a saturated calomel electrode (SCE). The counter electrode was a platinum gauze with a large surface area. All experiments were carried out at room temperature. Coulometric measurements were performed in a standard 20-mL cell. The working electrode was a glassy carbon tube (o.d. 5 mm) of 10-cm length. For the controlled-potential electrolysis, the anodic and cathodic compartments were separated by a fritted glass disk to prevent diffusion of the electrogenerated species. During the coulometric measurement of **3** in CH_3CN, a solid deposited onto the electrode. In dmf, no solid was formed, but the redox process was ill-defined.

X-ray Crystal Structure Determination: Single crystals of compounds **3**, **5** (Table 3), and **6** were selected and mounted onto a glass fiber. Compound **3** was placed in a cold nitrogen gas stream. **3:** Intensity data were collected with a Nonius-KappaCCD with graphite-monochromated Mo-K_α radiation. Determination of the unit-cell parameters, data collection strategy, and integration were carried out with the Nonius EVAL-14 suite of programs.[35] For compounds **5** and **6**, unit-cell dimensions and intensity data were collected with a Nonius CAD4-F diffractometer with graphite-monochromated Mo-K_α radiation. The unit-cell dimensions and crystal-orientation matrix were derived from least-squares refinement of setting angles of 25 reflections. Intensity data were collected by using the ω-2θ scan mode. The structures were solved by direct methods with the SHELXS-86 program[36] and refined by full-matrix least-squares methods with the SHELXL-97 software package.[37] CCDC-666581 and CCDC-666582 contain the supplementary crystallographic data for this paper. These data can be obtained free of charge from The Cambridge Crystallographic Data Centre via www.ccdc.cam.ac.uk/data_request/cif.

Table 3. Crystal data and structure refinement for compounds **3**, and **5**.

Compound	**3**	**5**
Empirical formula	$C_{72}H_{136}FeMo_6N_9O_{26}$	$C_{54}H_{96}N_4O_{23}V_6$
Formula mass	2175.39	1474.99
Temperature [K]	250	298
System	monoclinic	monoclinic
Space group	*C*2/*c*	$P2_1/c$
a [Å]	35.500(5)	11.436(5)
b [Å]	14.160(2)	16.184(5)
c [Å]	25.000(4)	18.627(7)
α [°]	90	90
β [°]	127.048(8)	97.65(3)
γ [°]	90	90
Volume [$Å^3$]	10 030(3)	3417(2)
Z	4	2
Parameters/restraints	470/16	397/53
Reflections collected/ unique	41900/13339	6677/6677
R_1 [I>2σ]	0.0634	0.0770
wR_2 (all data)	0.2379	0.2428
Goodness of Fit	1.036	0.991
CCDC-reference	666582	666581

Synthesis and Characterization

$[N(C_4H_9)_4]_3[FeMo_6O_{18}\{(OCH_2)_3CNHCO(4\text{-}C_5H_4N)\}_2]$ (3, Anderson-Fe-pyridine): $[N(C_4H_9)_4]_4[\alpha\text{-}Mo_8O_{26}]$ (1.00 g, 0.464 mmol, 1 equiv.), $Fe(acac)_3$ (0.246 g, 0.697 mmol, 1.5 equiv.), and **1** (0.370 g, 1.636 mmol, 3.5 equiv.) were introduced in a Schlenk tube under an argon atmosphere. Acetonitrile (35 mL) was added, and the resulting suspension was heated to reflux overnight under argon. The resulting solution was cooled to room temperature and centrifuged. The volume of acetonitrile was reduced to 15–20 mL, and the solution was exposed to vapors of diethyl ether. After three recrystallisations (from acetonitrile solutions exposed to ether vapors of diethyl), pale-yellow crystals were obtained (0.554 g, 43% yield based on Mo). $C_{68}H_{130}FeMo_6N_7O_{26}$ (2093.3): calcd. C 36.85, H 6.50, N 3.71; found C 36.58, H 6.57, N 3.34. IR: $\tilde{\nu}_{max}$ = 3426 (ν_{O-H}, s, br.), 2964–2875 (ν_{C-H}, s), 1667 ($\nu_{C=O}$, s), 1606 (w), 1542 (m), 1484 (δ_{C-H}, s), 1462 (m), 1422 (w), 1382 (m), 1324 (w), 1281 (w), 1222 (w), 1153 (w), 1103 (m), 1064 (w), 1029 (m), 941–923–90 ($\nu_{Mo=O}$, s), 853 (w), 807 (s), 756 (w), 664 ($\nu_{Mo-O-Mo}$, s), 560 (m), 485 (w), 415 (w), 372 (w), 313 (w) cm^{-1}. The paramagnetic nature of the compound prevents recording of NMR spectra.

$[N(C_4H_9)_4]_3[MnMo_6O_{18}\{(OCH_2)_3CNHCO(4\text{-}C_5H_4N)\}_2]$ (4, Anderson-Mn-pyridine): $[N(C_4H_9)_4]_4[\alpha\text{-}Mo_8O_{26}]$ (1.00 g, 0.464 mmol, 1 equiv.), $Mn(OAc)_3$ (0.188 g, 0.701 mmol, 1.5 equiv.), and **1** (0.370 g, 1.636 mmol, 3.5 equiv.) were introduced in a Schlenk tube under an argon atmosphere. Acetonitrile (35 mL) was added, and the resulting suspension was heated to reflux overnight under argon. The resulting solution was cooled to room temperature, centrifuged, and exposed to vapors of diethyl ether. After 4 h, the solution was again centrifuged, a white solid was discarded, and the solution was exposed to vapors of diethyl ether. After 2 d, orange crystals had formed (1.00 g, 78% yield based on Mo). $C_{68}H_{130}MnMo_6N_7O_{26}\cdot 3H_2O$ (2146.4): calcd. C 38.05, H 6.39, N 4.57; found C 37.98, H 6.47, N 4.47. IR: $\tilde{\nu}_{max}$ = 3446 (ν_{O-H}, s, br.), 3051 (w), 2962–2874 (ν_{C-H}, s), 1671 ($\nu_{C=O}$, s), 1601 (w), 1544 (m), 1485 (δ_{C-H}, m), 1409 (w), 1382 (w), 1324 (w), 1288 (w), 1220 (w), 1153 (w), 1099 (m), 1065 (w), 1026 (s), 942–921–903 ($\nu_{Mo=O}$, s), 848 (w), 810 (w), 757 (w), 667 ($\nu_{Mo-O-Mo}$, vs, br.), 566 (m), 520 (w), 462 (w), 411 (w), 366 (w), 321 (w) cm^{-1}. ^1H NMR (CD_3CN): δ = 64.5, 8.62 (br. s, 4 H), 7.59 (br. s, 4 H), 6.98 (br. s, 2 H), 3.11 (m, 24 H), 1.60 (m, 24 H), 1.35 (m, 24 H), 0.95 (t, J = 7.4 Hz, 36 H) ppm. ^{13}C NMR (CD_3CN): δ = 167.2, 150.8, 140.7, 123.1, 59.5, 24.5, 20.7, 14.2 ppm.

$[N(C_4H_9)_4]_2[V_6O_{13}\{(OCH_2)_3CCH_2OC(O)(4\text{-}C_5H_4N)\}_2]$ (5, Lindqvist-ester-pyridine): Decavanadate $[N(C_4H_9)_4]_3[H_3V_{10}O_{28}]$ (0.932 g, 0.553 mmol, 1 equiv.) and compound **2** (0.400 g, 1.658 mmol, 3 equiv.) were introduced in a Schlenk tube under an argon atmosphere. Acetonitrile (30 mL) was added, and the resulting solution was heated to reflux over 18 h, then cooled to room temperature, and filtered. An orange solid was isolated, and the filtrate was a green–brown solution. This solid was washed with acetonitrile (1 mL) and diethyl ether (15 mL), and the filtrate was a dark-green solution. The solid was dried to give **5** as an orange powder (0.487 g, 60% yield based on V). Single crystals suitable for X-ray diffraction were grown from a slowly cooling solution of **5** in acetonitrile. $C_{52}H_{96}N_4O_{23}V_6$ (1474.9): calcd. C 43.97, H 6.56, N 3.79; found C 43.73, H 6.78, N 3.77. IR: $\tilde{\nu}_{max}$ = 3447 (ν_{O-H}, s, br.), 2959–2874 (ν_{C-H}, m), 1735 ($\nu_{C=O}$, s), 1563 (w), 1470 (δ_{C-H}, m), 1405 (w), 1384 (w), 1323 (w), 1284 (ν_{C-O}, s), 1136 (m), 1061 (ν_{C-O}, s), 952 ($\nu_{V=O}$, s), 809 (ν_{V-O-V}, s), 757 (w), 721 (ν_{V-O-V}, s), 644 (w), 585 (m), 421 (m), 380 (w) cm^{-1}. ^1H NMR (CD_3CN): δ = 8.72 (d, J = 4.5 Hz, 4 H), 7.77 (d, J = 4.4 Hz, 4 H), 5.17 (s, 12 H), 4.22 (s, 4 H), 3.10 (m, 16 H), 1.61 (m, J = 7.5 Hz, 16 H), 1.34 (m, J = 7.3 Hz, 16 H), 0.96 (t, J = 7.0 Hz, 24 H) ppm. ^{51}V (CD_3CN): δ = –499 ppm.

$[N(C_4H_9)_4]_2[V_6O_{13}\{(OCH_2)_3CNHCO(4\text{-}C_5H_4N)\}_2]$ (6, Lindqvist-amide-pyridine): This compound was prepared in acetonitrile in varying yields. The procedure of Hill in dimethylacetamide (dma) reproducibly gave the desired compound in 40–45% yield. The analytical data corresponds to the literature values.

Complex 4-$[RuTPP(CO)]_2$: Anderson-Mn-pyridine **4** (8.8 mg, 4.2 μmol, 1.0 equiv.) and [RuTPP(CO)] (6.3 mg, 8.4 μmol, 2.0 equiv.) were dissolved in a mixture of $CHCl_3$ (0.6 mL) and CH_3CN (0.1 mL). The solution was gently heated until complete dissolution of the solid and stirred for 15 min at room temperature. A large excess of diethyl ether was added, and the resulting red precipitate was washed with diethyl ether and dried to give the title complex. $C_{158}H_{186}MnMo_6N_{15}O_{28}Ru_2$ (3576.0): calcd. C 53.07, H 5.24, N 5.87; found C 52.93, H 5.31, N 5.82. IR: $\tilde{\nu}_{max}$ = 3420 (ν_{O-H}, m, br.), 2960–2929–2873 (ν_{C-H}, m), 1951 [$\nu_{C\equiv O(Ru)}$, s, br.], 1682 [$\nu_{C=O(amide)}$, m], 1598 (w, Ru), 1529 (w), 1486 (δ_{C-H}, m), 1380 (w), 1351 (w, Ru), 1282 (w), 1178 (w, Ru), 1101 (m), 1072 (ν_{C-O}, m), 1029 (m), 1010 (s, Ru), 942–922–904 ($\nu_{Mo=O}$, s), 794 (w), 754 (w), 667 ($\nu_{Mo-O-Mo}$, vs, br.), 566 (m), 520 (w), 462 (w), 411 (w), 366 (w), 321 (w) cm^{-1}. ^1H NMR ($CDCl_3/CD_3CN$): δ = 64 (s br.), 8.45 (m, 16 H), 8.03 (d, J = 4.3 Hz, 8 H), 7.88 (d, J = 6.7 Hz, 8 H), 7.57 (m, 24 H), 5.22 (d, J = 5.2 Hz, 4 H), 2.87 (m, 24 H), 1.32 (m, 28 H), 1.11 (m, 24 H), 0.67 (m, 36 H) ppm. ^{13}C NMR ($CDCl_3$–CD_3CN): δ = 180.8 (C=O), 163.0, 144.0 (RuTPP), 143.5 (RuTPP), 142.4, 134.3 (RuTPP), 131.9 (RuTPP), 127.4 (RuTPP), 126.6 (RuTPP), 121.7, 119.7, 58.6 (TBA), 23.7 (TBA), 20.1 (TBA), 13.8 (TBA) ppm.

Complex 5-$[Ru(CO)TPP]_2$: In a Schlenk tube under an argon atmosphere, Lindqvist-ester-pyridine **5** (7.2 mg, 4.8 μmol, 1.0 equiv.) was suspended in $CHCl_3$ (5 mL, neutralized on alumina prior to use). [RuTPP(CO)] (7.2 mg, 9.7 μmol, 2.0 equiv.) was added, and the solution, which turns red and limpid, was stirred for 30 min and then exposed to vapors of diethyl ether. After 5 d, the resulting precipitate was washed with diethyl ether and dried to give the title complex. $C_{142}H_{152}N_{12}O_{25}Ru_2V_6$ (2958.6): calcd. C 58.46, H 5.17, N 5.68; found C 58.84, H 5.02, N 6.16. IR: $\tilde{\nu}_{max}$ = 3433 (ν_{O-H}, m, br.), 2956–2925–2855 (ν_{C-H}, m), 1970 [$\nu_{C\equiv O(Ru)}$, s], 1734 [$\nu_{C=O(ester)}$, m], 1598 (w, Ru), 1458 (δ_{C-H}, m), 1378 (m), 1352 (w, Ru), 1282 (m), 1175 (w, Ru), 1131 (m), 1065 (ν_{C-O}, m), 1008 (m, Ru), 954 ($\nu_{V=O}$, s), 809 (ν_{V-O-V}, s), 795 (m, Ru), 753 (m), 717 (m, Ru), 703 (m, Ru), 667 (w, Ru), 585 (w), 419 (w) cm^{-1}. ^1H NMR ($CDCl_3$): δ = 8.60 (s, 16 H), 8.20 (dd, J = 4.22 Hz, 8 H), 8.05 (dd, J = 5.48 Hz, 8 H), 7.70 (m, 24 H), 5.65 (d, J = 5.2 Hz, 4 H), 4.76 (s, 12 H), 3.60 (s, 4 H), 3.27 (m, 16 H), 1.63 (m, 16 H), 1.29 (m, 20 H), 0.73 (t, J = 7.4 Hz, 24 H) ppm. ^{13}C NMR ($CDCl_3$): δ = 175.5–144.0–143.8–142.8 (RuTPP), 134.3 (RuTPP), 131.9 (RuTPP), 127.4 (RuTPP), 126.6 (RuTPP), 59.0 (TBA), 24.4 (TBA), 19.8 (TBA), 13.8 (TBA) ppm.

Complex 6-$[Ru(CO)TPP]_2$: Lindqvist-amide-pyridine **6** (7.0 mg, 4.8 μmol, 1.0 equiv.) was dissolved in CH_3CN (1 mL). $CHCl_3$ (4 mL) and then [RuTPP(CO)] (7.4 mg, 9.9 μmol, 2.05 equiv.) were added. The solution, which turns red and limpid, was stirred for 2 h at room temperature. A large excess of diethyl ether was added, and the resulting red precipitate was washed with diethyl ether and dried to give the title complex (10 mg, 70%). $C_{142}H_{152}N_{14}O_{23}Ru_2V_6$ (2930.6): calcd. C 58.20, H 5.23, N 6.69; found C 58.63, H 5.41, N 6.82. IR: $\tilde{\nu}_{max}$ = 3438 (ν_{O-H}, m, br.), 2961–2931–2873 (ν_{C-H}, m), 1970 [$\nu_{C\equiv O(Ru)}$, s], 1685 [$\nu_{C=O(amide)}$, m], 1598 (m, Ru), 1529 (m), 1488 (δ_{C-H}, m), 1441 (m), 1352 (m, Ru), 1321 (w), 1306 (w), 1273 (w), 1176 (w, Ru), 1106 (m), 1070 (ν_{C-O}, m), 1009 (s, Ru), 955 ($\nu_{V=O}$,

s), 813 (ν_{V-O-V}, s), 795 (m, Ru), 753 (m), 717 (m, Ru), 703 (m, Ru), 667 (w, Ru), 644 (w), 585 (m), 420 (m) cm^{-1}. ^1H NMR (CD_3CN/$CDCl_3$): δ = 8.55 (s, 16 H), 8.15 (m, 8 H), 8.00 (m, 8 H), 7.71 (m, 24 H), 5.51 (d, J = 6.0 Hz, 4 H, H_{pyr}), 5.27 (s, 2 H, NH), 4.77 (s, 12 H), 3.27 (m, 16 H), 1.63 (m, 16 H), 1.45 (d, J = 6.0 Hz, 4 H, H_{pyr}), 1.29 (m, 20 H), 0.73 (t, J = 7.4 Hz, 24 H) ppm.

Complex 4-[ZnTPP]$_2$: Anderson-Mn-pyridine **4** (16.2 mg, 7.7 μmol, 1.0 equiv.) and [ZnTPP] (21 mg, 30 μmol, 4 equiv.) were dissolved in $CHCl_3$ (3 mL) and acetonitrile (1 mL). The solution was stirred at room temperature for 15 min, and a large excess of diethyl ether was added. The resulting precipitate was washed with diethyl ether and dried to give the title complex. $C_{156}H_{186}MnMo_6N_{15}O_{26}Zn_2$ (3448.6): calcd. C 54.33, H 5.43, N 6.09; found C 53.90, H 5.26, N 5.74. IR: $\tilde{\nu}_{max}$ = 3441 (ν_{O-H}, m, br.), 2960–2929–2873 (ν_{C-H}, m), 1654 (m), 1682 ($\nu_{C=O}$, m), 1598 (m, TPP), 1523 (w), 1486 (δ_{C-H}, m), 1440 (m), 1380 (w), 1339 (m, TPP), 1261 (w), 1204 (w), 1175 (w, TPP), 1068 (ν_{C-O}, m), 1029 (m), 1002–994 (s, TPP), 942–922–904 ($\nu_{Mo=O}$, s), 794 (m), 754 (m), 702 (m), 667 ($\nu_{Mo-O-Mo}$, vs, br.), 566 (m), 520 (w), 462 (w), 411 (w), 366 (w), 321 (w) cm^{-1}. ^1H NMR ($CDCl_3$/CD_3CN): δ = 63.5 (br. s), 8.75 (s, 16 H), 8.08 (d, J = 5.3 Hz, 16 H), 7.63 (m, 24 H), 5.95 (br. s, 4 H), 3.65 (br. s, 4 H), 2.96 (br. s, 24 H), 1.40 (br. s, 24 H), 1.17 (br. s, 24 H), 0.71 (br. s, 36 H) ppm. ^{13}C NMR ($CDCl_3$/CD_3CN): δ = 150.1, 144.8 ([ZnTPP]), 143.4 ([ZnTPP]), 134.6 ([ZnTPP]), 131.9 ([ZnTPP]), 127.4 ([ZnTPP]), 126.6 ([ZnTPP]), 120.7–120.6, 58.7 (TBA), 24.0 (TBA), 20.3 (TBA), 14.1 (TBA) ppm.

Supporting Information (see footnote on the first page of this article): Ligand syntheses, crystal data for **6**, further NMR spectra and fluorescence emission spectra of [ZnTPP] in the presence of **4** are presented.

Acknowledgments

This work would not have been possible without the inspiring scientific environment provided by Pierre Gouzerh, Anna Proust, and René Thouvenot, and we thank them very much. We also thank René Thouvenot for the ^{51}V NMR spectrum. We really appreciate the proofreading of the manuscript by Garry Hanan (University of Montreal), and we acknowledge helpful comments from the referees. The support of this research by the Agence Nationale pour la Recherche (ANR, project no. JC05_52436, post-doctoral fellowship to C. A.), by the CNRS, the Université Pierre et Marie Curie and the Université Paris Sud is gratefully acknowledged.

[1] a) R. Ballardini, P. Ceroni, A. Credi, M. T. Gandolfi, M. Maestri, M. Semararo, M. Venturi, V. Balzani, *Adv. Funct. Mater.* **2007**, *17*, 740–750; b) S. Saha, J. F. Stoddart, *Chem. Soc. Rev.* **2007**, *36*, 77–92.

[2] a) F. Scandola, C. Chiorboli, A. Prodi, E. Iengo, E. Alessio, *Coord. Chem. Rev.* **2006**, *250*, 1471–1496; b) Y. Kobuke, *Eur. J. Inorg. Chem.* **2006**, 2333–2351.

[3] a) H. Imahori, S. Fukuzumi, *Adv. Funct. Mater.* **2004**, *14*, 525–536; b) F. D′Souza, O. Ito, *Coord. Chem. Rev.* **2005**, *249*, 1410–1422.

[4] a) D. L. Long, E. Burkholder, L. Cronin, *Chem. Soc. Rev.* **2007**, *36*, 105–121; b) J. J. Borras-Almenar, E. Coronado, A. Müller, M. T. Pope (Eds.) *Polyoxometalate Molecular Science*, NATO Science Series Vol. 98, Kluwer Academic Publishers, Dordrecht, **2003**.

[5] N. Fay, V. M. Hultgren, A. G. Wedd, T. E. Keyes, R. J. Forster, D. Leane, A. M. Bond, *Dalton Trans.* **2006**, 4218–4227.

[6] a) A. Yokoyama, T. Kojima, K. Ohkubo, S. Fukuzumi, *Chem. Commun.* **2007**, 3997–3999; b) D. Attanasio, F. Bachechi, *Adv. Mater.* **1994**, *6*, 145–147; c) D. Hagrman, P. J. Hagrman, J. Zubieta, *Angew. Chem. Int. Ed.* **1999**, *38*, 3165–3168; d) A. Tsuda, E. Hirahara, Y.-S. Kim, H. Tanaka, T. Kawai, T. Haida, *Angew. Chem. Int. Ed.* **2004**, *43*, 6327–6331.

[7] a) A. Maldotti, A. Molinari, R. Argazzi, R. Amadelli, P. Battioni, D. Mansuy, *J. Mol. Catal. A* **1996**, *114*, 141–150; b) A. Molinari, R. Amadelli, V. Carassiti, A. Maldotti, *Eur. J. Inorg. Chem.* **2000**, 91–96; c) I. C. M. S. Santos, S. L. H. Rebelo, M. S. S. Balula, R. R. L. Martins, M. M. M. S. Pereira, M. M. Q. Simoes, M. G. P. M. S. Neves, J. A. S. Cavaleiro, A. M. V. Cavaleiro, *J. Mol. Catal. A* **2005**, *231*, 35–45; d) A. Maldotti, A. Molinari, P. Bergamini, R. Amadelli, P. Battioni, D. Mansuy, *J. Mol. Catal. A* **1996**, *113*, 147–157; e) A. Molinari, A. Maldotti, R. Amadelli, A. Sgobino, V. Carassiti, *Inorg. Chim. Acta* **1998**, *272*, 197–203.

[8] a) S.-Q. Liu, J.-Q. Xu, H.-R. Sun, D.-M. Li, *Inorg. Chim. Acta* **2000**, *306*, *87*–93; b) L. Gurban, A. Tézé, G. Hervé, *C. R. Acad. Sci. Paris, Série II* **1998**, 397–404.

[9] M. Bonchio, M. Carraro, G. Scorrano, A. Bagno, *Adv. Synth. Catal.* **2004**, *346*, 648–654.

[10] F. D′Souza, O. Ito, *Coord. Chem. Rev.* **2005**, *249*, 1410–1422.

[11] G. R. Newkome, G. R. Baker, S. Arai, M. J. Saunders, P. S. Russo, K. J. Theriot, C. N. Moorefield, L. E. Rogers, J. E. Miller, T. R. Lieux, M. E. Murray, B. Phillips, L. Pascal, *J. Am. Chem. Soc.* **1990**, *112*, 8458–8465.

[12] T. E. Stevens, *J. Org. Chem.* **1959**, *24*, 1715–1717.

[13] P. R. Marcoux, B. Hasenknopf, J. Vaisserman, P. Gouzerh, *Eur. J. Inorg. Chem.* **2003**, 2406–2412.

[14] S. Favette, B. Hasenknopf, J. Vaisserman, P. Gouzerh, C. Roux, *Chem. Commun.* **2003**, 2664–2665.

[15] Q. Chen, D. P. Goshorn, C. P. Scholes, X. L. Tan, J. Zubieta, *J. Am. Chem. Soc.* **1992**, *114*, 4667–4681.

[16] J. W. Han, K. I. Hardcastle, C. L. Hill, *Eur. J. Inorg. Chem.* **2006**, 2598–2603.

[17] B. Hasenknopf, R. Delmont, P. Herson, P. Gouzerh, *Eur. J. Inorg. Chem.* **2002**, 1081.

[18] A. Müller, J. Meyer, H. Boegge, A. Stammler, A. Botar, *Z. Anorg. Allg. Chem.* **1995**, *621*, 1818–1831.

[19] M. T. Pope, *Inorg. Chem.* **1972**, *11*, 1973–1974.

[20] L. Ruhlmann, A. Nakamura, H. Vos, J.-H. Fuhrhop, *Inorg. Chem.* **1998**, *37*, 6052–6059.

[21] M. Saito, A. Endo, K. Shimizu, G. P. Satô, *Electrochim. Acta* **2000**, *45*, 3021–3028.

[22] a) K. M. Kadish, D. Chang, *Inorg. Chem.* **1982**, *21*, 3614–3618; b) K. M. Kadish, D. J. Leggett, D. Chang, *Inorg. Chem.* **1982**, *21*, 3618–3622.

[23] A. Prodi, C. Chiorboli, F. Scandola, E. Iengo, E. Alessio, R. Dobrawa, F. Würthner, *J. Am. Chem. Soc.* **2005**, *127*, 1454–1462.

[24] S. S. Eaton, G. R. Eaton, *J. Am. Chem. Soc.* **1975**, *97*, 3660–3666.

[25] J. J. Bonnet, S. S. Eaton, G. R. Eaton, R. H. Holm, J. A. Ibers, *J. Am. Chem. Soc.* **1973**, *95*, 2141–2149.

[26] M. Nappa, J. S. Valentine, *J. Am. Chem. Soc.* **1978**, *100*, 5075–5080.

[27] C. H. Kirksey, P. Hambright, C. B. Storm, *Inorg. Chem.* **1969**, *8*, 2141–2144.

[28] A. S. Hinman, B. J. Pavelich, A. E. Kondo, S. Pons, *J. Electroanal. Chem.* **1987**, *234*, 145–162.

[29] A. Giraudeau, L. Ruhlmann, L. El Kahef, M. Gross, *J. Am. Chem. Soc.* **1996**, *118*, 2969–2979.

[30] a) G. H. Barnett, B. Evans, K. M. Smith, *Tetrahedron Lett.* **1976**, *44*, 4009–4012; b) D. Dolphin, D. J. Halko, E. C. Johnson, K. Rousseau in *Porphyrins Chemistry Advances* (Ed.: F. R. Longo), Ann Arbor Science: MI, **1979**, ch. 10; c) K. Rachlewicz, L. Latos-Grazynski, *Inorg. Chem.* **1995**, *34*, 718–727.

[31] a) L. Ruhlmann, A. Giraudeau, *Chem. Commun.* **1996**, 2007–2008; b) L. Ruhlmann, A. Giraudeau, *Eur. J. Inorg. Chem.* **2001**, 659–668.
[32] N. Hur, W. G. Klemperer, R.-C. Wang, in *Inorg. Synth.* Vol. 27 (Ed.: A. P. Ginsberg), John Wiley & Sons, New York, **1990**, p. 78.
[33] N. Hur, W. G. Klemperer, R.-C. Wang, in *Inorg. Synth.* Vol. 27 (Ed.: A. P. Ginsberg), John Wiley & Sons, New York, **1990**, pp. 83–85.
[34] B. Keita, K. Essaadi, L. Nadjo, *J. Electroanal. Chem. Interfacial. Electrochem.* **1989**, *259*, 127–146.
[35] A. J. M. Duisenberg, L. M. J. Kroon-Batenburg, A. M. M. Schreurs, *J. Appl. Crystallogr.* **2003**, *36*, 220.
[36] G. M. Sheldrick, *SHELXS-86*, University of Göttingen, **1986**.
[37] G. M. Sheldrick, *SHELXL-97*, University of Göttingen, Germany, **1997**.

Received: December 10, 2007
Published Online: April 17, 2008

